INTERNATIONAL JOURNAL OF HYDROGEN ENERGY 45 (2020) 2206–2223

Available online at www.sciencedirect.com

ScienceDirect

journal homepage: www.elsevier.com/locate/he

A systematic approach for matching simulated and experimental polarization curves for a PEM fuel cell

Muhammad Arif, Sherman C.P. Cheung, John Andrews *

School of Engineering, RMIT University, PO Box 71, Bundoora, 3083, VIC, Australia

HIGHLIGHTS

- Exchange current density and charge transfer coefficient affect activation losses.
- Effective water removal enhances PEM fuel cell performance at high currents.
- A systematic procedure is presented to match simulated and experimental V-j curves.
- Maximum percentage difference between simulation-4 and experimental data is 5%.
- The uniqueness of the best-fit input parameter values is discussed.

ARTICLE INFO

Article history:
Received 30 June 2019
Received in revised form
3 November 2019
Accepted 7 November 2019
Available online 6 December 2019

Keywords:
Simulation modelling
PEM fuel cells
ANSYS PEM Fuel Cell Module
Polarization curve
Matching simulated and experimental curves

ABSTRACT

Matching simulated and experimental polarization curves is an essential step in the modelling of polymer electrolyte membrane (PEM) fuel cells, but the numerical values of many input parameters like exchange current densities, charge transfer coefficients, protonic conduction coefficient and water removal coefficient are hard to be found experimentally. In this paper, the influence of these input parameters on the performance of PEM fuel cells has been investigated using the ANSYS PEM Fuel Cell Module. The simulation results show how the exchange current densities and charge transfer coefficients influence the activation losses; membrane resistance and contact resistance between the different components of a fuel cell contribute to the ohmic losses; and the coefficient of liquid water removal affects the concentration losses. A systematic procedure to match a simulated polarization curve with an experimental curve is presented and illustrated by application to an experimental PEM fuel cell with 5 cm^2 active area.

Introduction

To reduce global carbon dioxide emissions, dependence on fossil fuels needs to be reduced by utilising renewable energy sources for generation of electricity [1]. As a result of their intermittent nature, balancing demand and supply and ensuring continuous, reliable supply from renewable energy sources are major technical challenges requiring the development of a range of energy storage technologies [2]. Great efforts have been made to address these challenges, but amongst all electrical energy storage is the most promising solution [3]. Hydrogen gas produced from renewable energy, stored and then reconverted back into electricity in a PEM fuel

* *Corresponding author.*
E-mail addresses: muhammad.arif@student.rmit.edu.au (M. Arif), chipok.cheung@rmit.edu.au (S.C.P. Cheung), john.andrews@rmit.edu.au (J. Andrews).
https://doi.org/10.1016/j.ijhydene.2019.11.057

cell is an increasingly important option for storing electricity [4].

Fabrication and testing of PEM fuel cell prototypes takes considerable time and is costly [5]. Hence, instead of laborious and costly experiments, Computational Fluid Dynamics (CFD) coupled with a 3D electrochemical and electric field – current density modelling have been increasingly used for modelling and performance assessment of PEM fuel cells by running numerical simulations [6]. Besides analysing PEM fuel cell performance, it is also imperative to understand the local processes that take place within the cells [7]. Two fundamental phenomena in PEM fuel cells are water management and thermal management, which are impossible to study *in situ* within the compact and closed structure of a cell. The best way of understanding these processes is thus by modelling and simulation [8] with constant reference to experimental data at the aggregate level, that is, local current and mass flow rates. The challenges faced by researchers in investigating these processes solely through experiments have motivated development of computational models for PEM fuel cells. Modelling can be further used as a tool to diagnose the factors limiting the performance of PEM fuel cell and optimise its performance.

The modelling of PEM fuel cells started with one-dimensional models, which was later extended to 2D and 3D. Validation is an essential step in CFD –based fuel cell simulations, in which the results of the simulation are compared with experimental results [9]. Most researchers have compared the model's simulated polarization curves with the experimental curves and found close agreement but with some discrepancies.

Bernardi et al. [10] developed a one-dimensional (in the flow direction) mathematical model for a solid polymer electrolyte fuel cell to find out the factors affecting the cell performance and explain the transport mechanism of species. The value of exchange current density was used as a fitting variable to get the best fit between the model and experimental results, but exchange current density is a function of temperature and Pt loading.

Thomas and John [11] extended computational simulation of fuel cells to a 2D mathematical model for a solid polymer electrolyte fuel cell, by representing the membrane electrode assembly in two dimensions to analyse water management, thermal management and hydrogen consumption. The sharp turn down due to mass transport limitations, was not observed in model's polarization curve until the value of current density reached 5 A/cm^2, because their model did not consider the mass transport losses due to the adsorption and transport of reactants and oxidants in ionomer film and water.

Jung S and Trung V [12] built a 2D along-the-channel model to investigate the influence of different channels configuration and operating parameters on the performance of PEM fuel cell using two dimensional along the channel model. The model could not predict the sharp turn down in cell voltage at high current densities due to mass transport limitations, because their model did not include the resistance to the gasses flowing through porous electrodes.

Later Mazumder and Cole [13] developed a 3D model with governing equations for formation and transport of liquid water within PEM fuel cell. The results obtained from the model over-predicted the experimental results due to neglecting factors like the dissolution of species gases in the liquid, Knudsen diffusion, clogging of active reaction sites on catalyst layers due to the formation of liquid water, etc.

Moein-Jahromi and Kermani [14] used the agglomerate model to simulate the cathode catalyst layer of a PEM fuel cell and compare the results with homogenous cathode catalyst model. It was observed that the homogeneous model over-predicted the experimental results by around 80% while the agglomerate model has a good agreement.

Xing, Mamlouk and Scott [15] developed a 2D steady state isothermal model to study the effects of platinum and carbon loading on the performance of the PEM fuel cell. According to the modelling results, the sharp turn down at high current densities is due to an increase in resistance to the diffusion of oxygen through water film.

Limjeerajarus and Charoen-Amornkitt [16] investigated the influence of channel flow configurations and number of channels on the performance of the PEM fuel cell. The modelling results reported a reasonable agreement between experimental data and simulation results with a small difference due to exchange current density evaluation.

Macedo-Valencia et al. [17] developed their models to study the performance of five cells PEM fuel stacks. The values used for the physical properties of MEA were slightly different from experimental values, which caused a difference in the simulation and experimental data.

Heidary et al. [18] investigated the influence of inline and staggered blockages in the parallel channels configuration and then compared with the performance of parallel channels without blockage. The simulated polarization curve was compared with the experimental polarization curve for the model validation. A reasonable agreement was found between the two polarization curves with some differences. The difference in the performance was due to some assumptions made in the model.

Chowdhury, Genc and Toros [19] developed a 3D single phase isothermal model to optimise the channel to land width ratio of the PEM fuel cell. The model was validated by comparing the model and experimental polarization curves, and excellent agreement found between the both results with less than 1% difference.

Havaej et al. [20] developed a 3D two-phase model to investigate the effects of catalyst loading distribution on the performance of PEM fuel cell. The simulated polarization curve was compared with experimental polarization curve for two different operating conditions. The numerical results obtained from the model presented in the paper was in a good agreement with experimental results under both operating conditions.

Li and Sundén [21] studied the influence of GDL deformation on the transport phenomena and PEM fuel cell performance by developing a 3D, non-isothermal, two-phase mathematical model. The accuracy of the mathematical model was assessed by comparing numerical model's polarization curve with the experimental polarization curve form the literature. The results of mathematical model were in a reasonable agreement with the experimental results.

Carcadea et al. [22] investigated the influence of catalyst layer composition and properties (like; platinum loadings,

ionomer volume fraction, particle radius and electrochemical active surface area) and the mass transport resistance due to ionomer and liquid water covering catalyst particles, on the performance of the PEM fuel cell. The model results showed that lower particle radius and high platinum loadings can result in high cell performance. The results of numerical model were validated with experimental data and good agreement was found between the results.

According to Bednarek and Tsotridis [6,9], one of the reason for not obtaining accurate results from simulation is lack of robust and reliable data for various input parameters like; exchange current densities, open cell voltage, charge transfer coefficients and etc. In the literature the range of values for exchange current densities and charge transfer coefficients are very broad. There is no clear guide about the range for the values of exchange current densities and charge transfer coefficients. Zalitis et al. [23] had compared a broad range of exchange current densities values at different conditions obtained from the literature. Similarly, no range of values has been found in the open literature for the value of coefficient of liquid removal.

Harvey, Pharoah and Karan [24] used a 3D CFD model to compare different approaches used for modelling of catalyst layers in the PEM fuel cell. The study pointed out that a large number of CFD models used for modelling of fuel cells do not include catalyst agglomerate model due to which sharp turn down due to mass transport losses at higher current densities is not observed. Same discrepancies were found by Jung S and Trung V [12] and Mazumder and Cole [13] while validating their models against the experimental data. In the agglomerate catalyst model, the catalyst layer is assumed to be made up of many agglomerates, each of consisting of carbon black particles and platinum catalysts dispersed on its surface.

Ju and Wang [25] found a very good agreement between the simulated and experimental polarization curves, but the agreement between simulated and experimental at current distribution level for the same input parameters values was not satisfactory. This concluded that by just comparing simulated and experimental global polarization curves is inadequate for the PEM fuel cell model validation. Lum and McGuirk [26] validated their model by comparing numerical and experimental local current distribution data. Such data on the spatial distribution of current density was not obtainable in our experimental cell, and indeed is generally not obtainable without a highly specialised experimental set up and test cell.

The experimental data for the local distribution of current density and species gasses are not generally available. A highly specialised experimental setup, as used by Ref. [27] is required to obtain the experimental data for the local distribution of current density and species gasses. So as a result, in the open literature, most of the researchers have compared the model's global polarization curves with the experimental polarization curves to assess the accuracy of their models as mentioned by Ref. [21].

Various commercial softwares like ANSYS Fluent, Open FOAM, STAR-CD, and COMSOL have been used for modelling and simulation of fuel cells over the fifteen years. Despite the availability of several simulation packages for PEM fuel cells, a step-by-step procedure for matching a simulated polarization curve to an experimental curve has so far not been articulated. This is the task taken up in the present paper, with reference to a 5 cm^2 PEM fuel cell with a parallel channel configuration for which experimental polarization curves under various conditions have been obtained. A cell with the same dimensions and component properties has been simulated using the ANSYS PEM Fuel Cell Module. The equations used for modelling electrochemistry, current and mass transport, and the formation and transport of liquid water have been studied in detail.

The values of the model input parameters like exchange current density, charge transfer coefficient, membrane protonic conduction coefficient, and liquid removal coefficient are systematically varied to investigate their impacts on the different regions of the polarization curve, and hence achieve a close fit to the experimental polarization curve. On the basis of this analysis, a detailed step-by-step procedure to match a simulated and experimental curve is formulated to calibrate the embedded empirical parameters to capture the fuel cell characteristics accurately.

It should be noted that the model calibration procedure used here is simply relying on matching experimental and simulated polarization curves. These V–j curves are extracted from the model by integrating current density over the entire active area. We are assuming that the detailed equations in the simulation model that are solved numerically in each small elemental volume over the 3D space occupied by the cell – which are all based on accepted classical electrostatic and fluid dynamics theory – are accurately representing the spatially-disaggregated physical and electrochemical processes taking place.

The influence of input parameters on a polarization curve

Model description

The ANSYS PEM Fuel Cell Module is an add-on module to the ANSYS Fluent CFD software that has the capability of modelling electrochemistry, current and mass transport, formation and transport of liquid water, and heat sources in PEM fuel cells [28]. The ANSYS PEM Fuel Cell Module has been selected for the present study because it has the capability of full 3D modelling of all components in fuel cell, so it can completely represent the geometry and structure of an actual experimental fuel cell, and the properties of different components [29]. Moreover, Fluent can solve the basic governing equations required to model the PEM fuel cell solely.

The ANSYS PEM Fuel Cell Module has undergone significant revisions since first introduced. In the latest versions (ANSYS 17.0 and subsequent), the new PEM Fuel Cell Module included the agglomerate catalyst model, along with several other modifications compared to the old module [28]. As mentioned by Ref. [24], unlike the thin-interface and discrete volume catalyst models, the agglomerate catalyst model is capable of modelling the mass transport losses due to the dissolution of oxygen in the ionomer.

This ANSYS PEM Fuel Cell Module uses equations that are based on conservation of mass, conservation of charge,

species transport, conservation of momentum, and conservation of energy. The principal assumptions that are made in the Module for current study are:

- laminar flow
- non-isothermal
- steady state
- reactants and oxidants obey ideal gases laws
- materials of catalyst, GDLs and membrane are isotropic
- liquid water formation is included.

ANSYS PEM Fuel Cell Module setup

A 5 cm^2 PEM fuel cell was created in the SolidWorks exactly with the same dimensions as actual test cell. The actual test cell and the test bench are shown in Fig. 1 [29], and Fig. 2 [29], respectively. The dimensions of the cell components are listed in Table 1.

After creating geometry, the next step is to discretise the geometry into small cells which is called meshing. The simulation of PEM fuel cell requires a mesh that receives a converged solution in less computational time. The edge sizing for each edge of bipolar plates and gas flow channels were set 0.5 mm. Similarly, the size of each element on the length and width of the membrane, GDLs and catalyst layers were also set to 0.5 mm.

A grid independent analysis has been done to keep balance between the accurate results and computational time. The number of grid layers along the MEA was varied and simulated for one voltage point to check the difference in the results for different number of grid layers.

The total number of elements was increased as the number of grid layer increased along MEA (i.e.: membrane, catalyst layer and GDL). Three different sets of numbers of grid layers within the membrane-CL-GDL structure – i.e.; 6-4-6, 8-6-8 and 10-8-10 respectively were analysed to check the mesh sensitivity. The total numbers of elements in the model for the 6-4-6 membrane-CL-GDL structure was 344318; for the 8-6-8 structure, 364558; and for the 10-8-10 structure, 384798. As it can be seen from Fig. 3, the values of current densities for all grid layers are almost the same, but by increasing the number of grids layers the computational time increases significantly. So, to reduce the computational time without affecting the accuracy of the results, the mesh with 6-4-6 number of grid layers was finalised for all simulations.

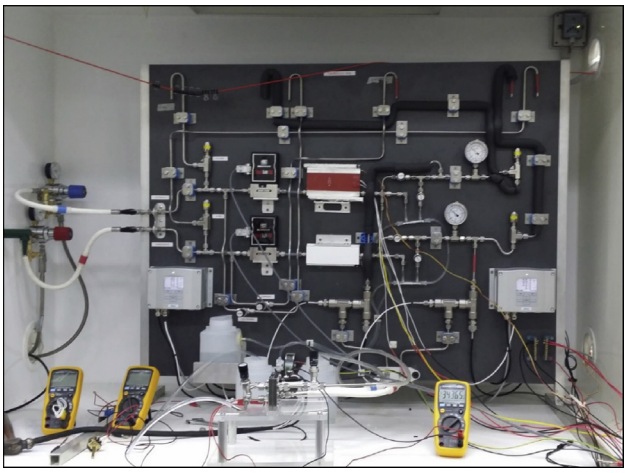

Fig. 2 – A test rig for URFC in the Sustainable Energy Hydrogen Lab at RMIT Bundoora East campus [29].

Table 1 – Model geometry parameters.

Parameter	Value	Unit	Reference
GDL anode thickness	0.30	mm	From experimental cell
GDL cathode thickness	0.27	mm	From experimental cell
Catalyst layer thickness	0.02	mm	From experimental cell
Bipolar plates thickness	3	mm	From experimental cell
Channel width	1	mm	From experimental cell
Channel height	1	mm	From experimental cell
Active area	500	mm^2	From experimental cell

After that the mesh was imported into ANSYS FLUENT for simulation using ANSYS PEM Fuel Cell Module. The material properties of membrane, GDL and catalyst layers used in the simulations are listed in Table 2.

The boundary conditions applied were the same as used during experimental cell testing (Table 3). A pressure-velocity coupling solution method with SIMPLE scheme were used for simulations in this study. A first-order upwind spatial discretization scheme was applied to density, momentum, species, energy, water content, electrical potential, protonic potential, water content and liquid saturation in the channels.

An accurate convergence criterion is needed for every simulation to get precise results. Therefore in this study, the four convergence criteria suggested by Ref. [30] were used for simulations which include calculating of current at terminals,

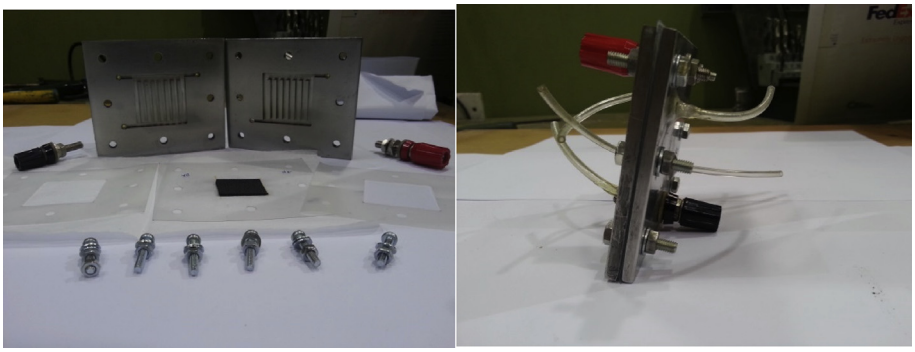

Fig. 1 – Experimental PEM fuel cell with parallel channels configuration [29].

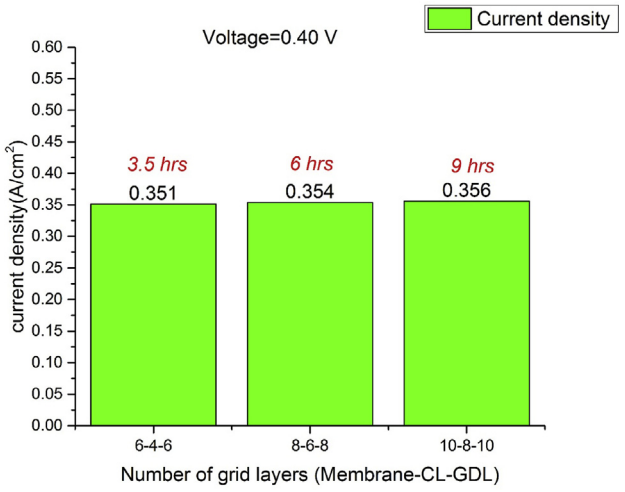

Fig. 3 – Grid independent analysis of the mesh.

Table 2 – Material properties of cell MEA components.

Physical parameters	Value	Units	Reference
Membrane	**NAFION 115**		
Dry membrane density	1968.5	Kg/m^3	Manufacturer data sheet
Thermal conductivity	2	W/m.K	Manufacturer data sheet
Electrical conductivity	1 E^{-16}	Simens/m	Manufacturer data sheet
GDL-anode	**Elat-elt1400w**		
Density	377	Kg/m^3	Manufacturer data sheet
Thermal conductivity	2	W/m.K	Manufacturer data sheet
Electrical conductivity	267059	Simens/m	Manufacturer data sheet
Porosity	0.63		Manufacturer data sheet
Contact angle	130	degrees	calculated
GDL-cathode	**Sintered Titanium**		
Density	1351.8	Kg/m^3	Manufacturer data sheet
Thermal conductivity	21.9	W/m.K	Manufacturer data sheet
Electrical conductivity	2380000	Simens/m	Manufacturer data sheet
Porosity	0.63		Manufacturer data sheet
Contact angle	70	degrees	calculated
Catalyst layer			
Porosity	0.28		[29]
Contact angle	130	degrees	calculated
Catalyst loading anode PtB	4	mg/cm^2	Manufacturer data sheet
Catalyst loading cathode PtB/IrO_2	4	mg/cm^2	Manufacturer data sheet

Table 3 – List of operating conditions for test cell.

Operating condition	Value
Cell Temperature	53 C°
Relative Humidity at anode	66%
Relative Humidity at cathode	34%
Inlet mass flow rate of hydrogen at anode	3 E^{-09} kg/s
Inlet mass flow rate of air at cathode	8.20 E^{-07} kg/s

calculating the consumption of species, checking the reported current density and checking the current densities are not changing with further iterations. The simulation output value of current at the cathode terminal was compared with the calculated value of the current from the oxygen consumption. The solution was considered to be converged if the difference between the values of current at cathode terminal and calculated from the oxygen consumption was less than 0.0001. Similarly, the simulations were stopped when the difference in the reported current densities between iterations was less than 0.0001 for the same voltage point.

Polarization regions of PEM fuel cell polarization curve

The polarization curve of a PEM fuel cell can be categorised into three distinct regions based on the causes of potential loss; activation, ohmic and concentration (Fig. 4) [31].

At lower current densities, the voltage drops due to the activation energy required for the electrochemical reaction at the catalyst surface. The lower this energy is, the more effective is the catalyst. The initial rapid drop region of the polarization curve is called activation polarization region. Charge transfer coefficient and the exchange current densities are affecting the activation polarization region of the curve.

At medium current densities, the cell voltage drops linearly with current due to ohmic losses. These losses occur due to the electrical resistance in different components of fuel cell like; membrane, catalyst layers, GDLs and bipolar plates. The linear drop region due to the electrical resistance of different fuel cell components is called the ohmic polarization region. Protonic conduction coefficient and contact resistivity are the model input parameters that influence the curve in this region.

At high current densities, the rate of water generation increases at cathode electrode and causes flooding. Through water flooding, the pores of the electrode are blocked with water that minimises the flow of oxidants into the catalyst layer, due to which less current is generated at a given voltage. This drop in performance causes a sharp turn down in the polarization curve, which is called the concentration polarization region. The concentration losses can be reduced by effective water removal. Hence the input parameter that impacts the concentration losses is coefficient of liquid water.

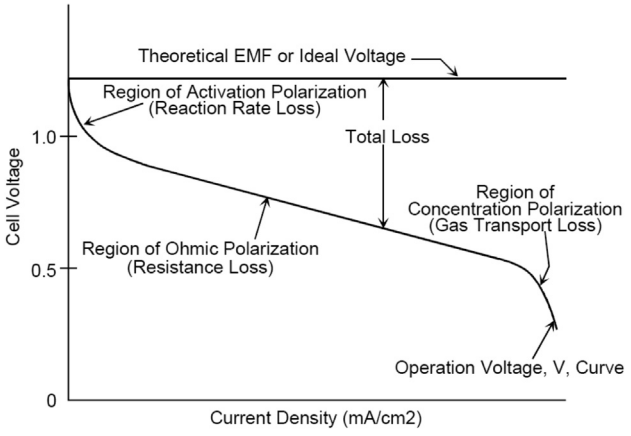

Fig. 4 – Polarization curve of a PEM fuel cell [31].

In the next sub-sections, a 5 cm^2 PEM fuel cell with parallel flow channels is simulated using the ANSYS PEM Fuel Cell Module with varying input parameters, including: exchange current densities, charge transfer coefficients, protonic conduction coefficient and water removal coefficient. Over the past few years some researchers (e.g. Refs. [32–34], have studied the influence of various input parameters on the polarization curve of a PEM fuel cell. In the present study, the sensitivity analysis of the input parameters such as exchange current densities, charge transfer coefficients, protonic conduction coefficient and water removal coefficient is performed to investigate the effect of these parameters on each region of the polarization curve – i.e.: the activation polarization, ohmic and mass transport losses regions. The analysis performed is used in developing for the first time a detailed step-by-step procedure to match a simulated and experimental polarization curves. It is important to note that the influence of the values of coefficient of liquid removal on the polarization curve has not been investigated in the past studies. In addition, the ANSYS PEM Fuel Cell Module has gone through vast modification and improvements over time, especially compared to the study performed by Ref. [32]. Hence it is necessary to check the sensitivity of these input parameters using the updated version of ANSYS PEM Fuel Cell Module for developing systematic procedure to match numerical and experimental polarization curves.

One input parameter is varied at a time while keeping other input parameters constant to analyse the individual effect of each input parameter on the simulated polarization curve. The cell operating conditions are the same for all these simulations and are taken from actual experimental results (see Table 3).

Charge transfer coefficients

The amount of the potential energy applied to an electrochemical reaction that enhances the rate of reaction is called charge transfer coefficient [35]. The charge transfer coefficient is generally a function of operating parameters like temperature and material properties of the electrode. Tijani, Binti Kamarudin and Binti Mazlan [36] and Biaku et al. [35] found that the value of the charge transfer coefficient increases with an increase in the operating temperature. Soderberg et al. [37] investigated the influence of the properties of a porous electrode on the value of charge transfer coefficient. It was found that the value of charge transfer coefficient increases with an increase in electrode porosity while it decreases with increase in the thickness of electrode layers.

The volumetric transfer current ($\mathscr{R}$) terms are source terms that are described in the PEM Fuel Cell Module [28] by Butler-Volmer equation as:

$$R_{an} = \left(\zeta_{an} j_{an}(T)\right)\left(\frac{[A]}{[A]_{ref}}\right)^{\gamma_{an}}\left(-e^{+\alpha_{an}^{an} F \eta_{an}/RT} + e^{-\alpha_{cat}^{an} F \eta_{an}/RT}\right) \quad (1)$$

$$R_{cat} = \left(\zeta_{cat} j_{cat}(T)\right)\left(\frac{[C]}{[C]_{ref}}\right)^{\gamma_{cat}}\left(-e^{+\alpha_{an}^{cat} F \eta_{cat}/RT} + e^{-\alpha_{cat}^{cat} F \eta_{cat}/RT}\right) \quad (2)$$

All the parameters listed above, excluding Faraday and universal gas constant, are input parameters and can be varied to get the best match with experimental results. There are four different charge transfer coefficients, which have different values that can be separately set as an input to get a good fit with the experimental polarization curve, especially in the activation polarization region. This has emerged from the work done by Wu [29].

From the Butler-Volmer equation, the charge transfer coefficients have an exponential effect on the current density. By increasing the value of charge transfer coefficients, the current density increases for the given voltage. As the voltage decreases, the current density rises more by increasing the charge transfer coefficient, this because the charge transfer coefficient is multiplying with the overpotential value in the Butler-Volmer equation. The values for charge transfer coefficients were changed in two different ways: first the value of one coefficient was varied while keeping other same; and then values for both coefficients were changed together.

To explore the effect of charge transfer coefficients on a polarization curve, simulations for the 5 cm^2 test cell described above were run first by varying the value of one coefficient while keeping the other same; and secondly by changing the values of both coefficients together.

The simulated polarization curve for the first set of runs is displayed in Fig. 5a. When the value of the charge transfer coefficient of the cathode has increased the values of current densities increases significantly. While on the other side, by increasing the values of the anode charge transfer coefficient while keeping the values of charge transfer coefficients for cathode constant, the rise in current density values is negligible. The change in values of cathodic charge transfer coefficient is more effective because the overpotential at the anode is almost insignificant compared to the cathode [38], and charge transfer coefficient is multiplied with the surface overpotential in the Butler-Volmer equation. Similar trend was found in the study conducted by Ref. [32].

For the second case, it can be seen from the polarization curves obtained from simulation results in Fig. 5b that current density increases by increasing the value of charge transfer coefficients. Polarization curves with high charge transfer coefficients (0.7, 0.8) are getting closer to a straight line, especially at high current densities. Meanwhile for the lower charge transfer coefficients (0.4), the curve tends to turn down steeply. It can be observed in both cases that by increasing the value of charge transfer coefficients the slope (negative) of the curves decreases in all the regions.

Exchange current densities

Exchange current density is a parameter that estimates the ability of an electrode to undergo an electrochemical reaction. A higher value of the exchange current density indicates that the electrode's surface is highly active for the electrochemical reaction. For a PEM fuel cell, the value of the overpotential at the anode electrode is almost negligible in comparison to the cathode electrode. Since the total current density at both electrodes must be equal by conservation of charge, the value of exchange current density at the anode must be several orders of magnitude larger than the at the cathode [38]. Different materials have different values of exchange current density. Platinum has the highest value (10^{-3} A/cm^2) making it most

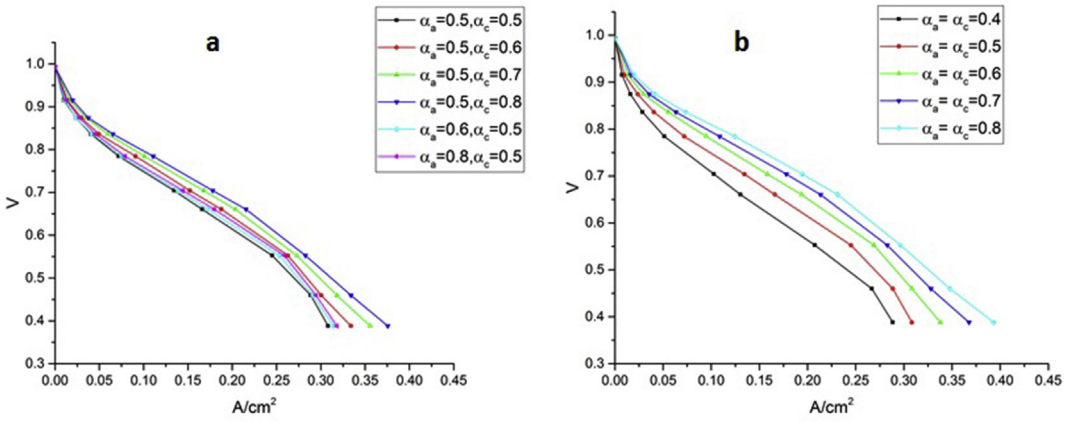

Fig. 5 – Comparison of simulated polarization curves for different values of charge transfer coefficient on anode and cathode electrodes.

favourable as a catalytic material, but it is very expensive. In the literature, a large variability is found in the range of the values of exchange current density even for the same material. Therefore, most researchers use it as a fitting parameter to match a simulated curve with experimental data.

From Butler-Volmer Eqs. (1) and (2), by increasing the value of exchange current densities, the value of the current density increases for the same voltage. By increasing the value of the exchange current density, the activation losses decline, and high current is generated for the small values of overpotential, showing that the catalytic surface is favourable for rapid electrochemical reaction to occur. Exchange current densities reflect the importance of catalyst selection in a PEM fuel cell.

The 5 cm^2 PEM fuel cell operating under the same conditions was simulated for three different values exchange current densities on each electrode while all other input parameters were constant. Fig. 6 shows the polarization curves obtained from the simulation for three different sets of values of exchange current densities. As expected from

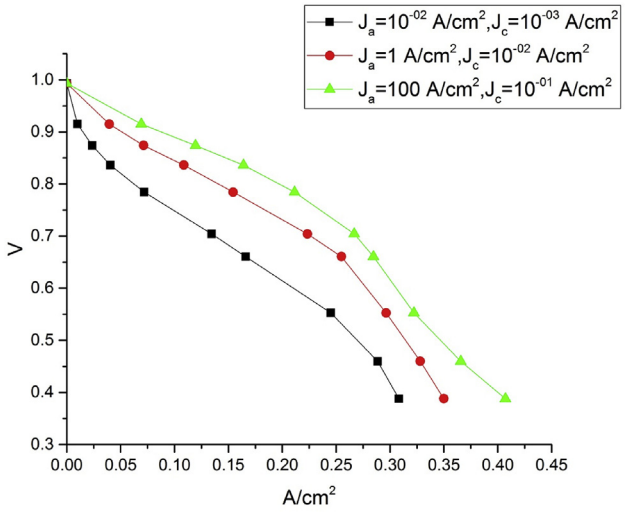

Fig. 6 – Comparison of polarization curves for different values of exchange current densities on anode and cathode electrodes.

Butler-Volmer Eqs. (1) and (2), the catalyst with the high value of exchange current density will produce high current compared to the catalyst with the lower value of exchange current density at same voltage drop. As can be seen in Fig. 6, with an increase in the values of exchange current densities the values of output current densities increase by a significant amount even at low values of overpotential. These results indicate that a better performing catalyst can reduce the activation losses, which will result in the better performance of the cell.

Protonic conduction coefficient

The driving force behind the electrochemical reactions taking place at anode and cathode catalysts is the potential difference between the solid phase (GDL catalyst layers and end plates) and membrane phase (membrane and catalyst layer). The ANSYS PEM Fuel Cell Module [28] uses conservation of charge equations to solve for the two potentials – electronic and protonic potentials.

$$\nabla \cdot (\boldsymbol{\sigma}_{sol} \nabla \phi_{sol}) + R_{sol} = 0 \tag{3}$$

$$\nabla \cdot (\boldsymbol{\sigma}_{mem} \nabla \phi_{mem}) + R_{mem} = 0 \tag{4}$$

The membrane phase conductivity is modelled by equation:

$$\boldsymbol{\sigma}_{mem} = \boldsymbol{\beta}_i (0.514\lambda - 0.326)^{\omega} e^{E_i \left(\frac{1}{303} - \frac{1}{T}\right)} \tag{5}$$

The polymer electrolyte membrane used in a PEM fuel cell allows only protons to pass through it. The proton conductivity mainly depends on the water content in the membrane. The higher the water content, the higher will be the conductivity and vice versa. The protonic conduction coefficient (β_i) is a numerical constant that must be input to the model used in ANSYS fluent for generality. It can be used as a fitting variable to get the best match between the simulated and experimental curves.

The test cell defined in section Polarization regions of PEM fuel cell polarization curve was simulated for three different

values of protonic conduction coefficient (β_i) under the same operating conditions while keeping other input parameters constant. As can be anticipated from Eq. (5), the polarization curves obtained from the simulation are raised in the ohmic polarization portion by increasing the value of protonic conduction coefficient (Fig. 7), thus reflecting the lower membrane resistance and improved performance. Two criteria can be used to check the valid range for the protonic conduction coefficient. Firstly, the value of membrane conductivity calculated from the simulation output values should be compared with the membrane conductivity value reported by literature. Secondly, the membrane resistance should not be greater than the value of total cell resistance as measured in an experimental cell.

Contact resistance

The total fuel cell resistance is the sum of the membrane resistance and contact resistances between different components of the fuel cell, assuming the electrical resistance of the GDLs and endplates are negligible compared to the contact resistance and membrane resistance. This assumption is made because the value of electrical conductivities for GDLs materials are very high as it can be seen in Table 2. The primary source of the contact resistance in a fuel cell is the resistance at the interface between GDL and bipolar plates. The contact resistance depends upon the electrical conductivity of components and the clamping pressure. The contact resistance decreases as the clamping pressure increases, but very high clamping pressure may damage the MEA. The contact resistance between different components can be reduced by applying optimal clamping pressure. Mishra, Yang and Pitchumani [39] found that cloth based GDLs have lower values of contact resistance than the paper-based GDLs.

The test PEM fuel cell described in section Polarization regions of PEM fuel cell polarization curve was simulated using the ANSYS PEM Fuel Cell Module for two different cases: without and with contact resistivity of 11.5 E^{-06} Ω-m^2. The polarization curves obtained from the simulation results are shown in Fig. 8. As expected, including the contact resistance led to a drop in current density in the ohmic region of the polarization curve.

Coefficient of liquid removal

The rate of water generation at the cathode is directly related to the current produced. From the ANSYS PEM Fuel Cell Module [28], the water produced due to oxygen reduction reaction is:

$$S_\lambda = \frac{M_{w,H_2O}}{2F} R_{cat} > 0 \quad (6)$$

At high current densities, the rate of water generation increases, which results in the clogging of pores of GDL. The clogging of pores minimises the flow of oxidants to the catalyst, which limits the performance of fuel cell due to mass transport losses. Most of the models quantify the generation of liquid water as liquid saturation or volume fraction of liquid water "s". Liquid saturation is a ratio of the volume of water inside the pores to the volume of pores. The term "s" is a critical parameter for modelling of mass transport losses in PEM fuel cells. This parameter also works as an indicator of how much the flow of species is restricted due to liquid water formation. The blockage of GDL pores due to liquid water is more severe on the cathode side, because water is mainly generated at the cathode side.

The ANSYS PEM Fuel Cell Module [28] models the drop in performance of a PEM fuel cell due to clogging of GDLs and catalyst pores by liquid water "s" as follows:

$$D_{eff}^{ij} = (1 - s)^{r_s} \varepsilon^{1.5} D^{ij} \quad (7)$$

$(1 - s)^{r_s}$ is the pore blockage term due to liquid water, r_s is

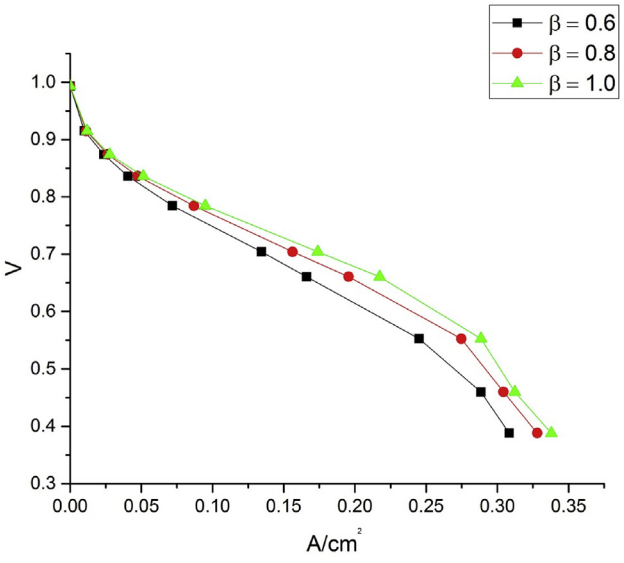

Fig. 7 – Comparison of polarization curves for the test cell for different values of protonic conduction coefficient of membrane.

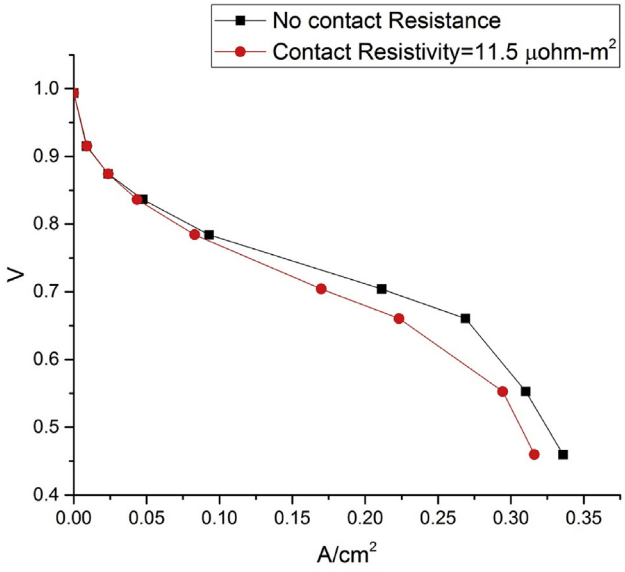

Fig. 8 – Comparison of simulated polarization curves for the test for different values of contact resistance.

the exponent of pore blockage, which shows the effect of liquid water on the blockage of pores of electrodes and GDLs.

The gas species diffusivity "D^{ij}" term in Eq. (7) is evaluated with respect to individual species based on operating conditions by the full multicomponent diffusion method. The gas diffusion coefficient governs the diffusion rate of the gas species.

The liquid water can also cover the active sites of catalysts and thus reducing the effective surface area of the catalyst layer for the electrochemical reaction.

$$R_j = (1 - s)^{\gamma_j} R^0_{cat} \tag{8}$$

$(1 - s)^{\gamma_j}$ is the term that shows the reduction of catalyst effective surface area due to liquid water.

The liquid water generated at the cathode as a result of the electrochemical reaction is driven out of the GDL to channels by capillary pressure [28].

$$f_{liq} = \Theta \varepsilon s . \max\left[\left(p_c + \frac{1}{2}\rho V^2\right), 0\right] \tag{9}$$

The rate of water removal depends on the porosity of GDL, capillary pressure and the coefficient of liquid removal. By decreasing the value of the coefficient of liquid removal, more liquid water will remain inside the pores of GDL and electrode, which will minimise the supply of oxidants to the catalyst and less current will be produced.

The test cell operating at the same conditions was simulated for two different values of liquid removal coefficient while all other input parameters were held constant. The simulation results show that the cell with the high value of the coefficient of liquid removal (5 E^{-05} s/m) has performed better in the concentration losses region compared to the cell with a low value of the coefficient of liquid removal (5 E^{-15} s/m) as depicted in Fig. 9. The concentration losses can be reduced by increasing the value of the coefficient of liquid removal and vice versa. One point that is worth noting is that concentration losses begin at medium current densities and get more with an increase in current densities, as shown in Fig. 9.

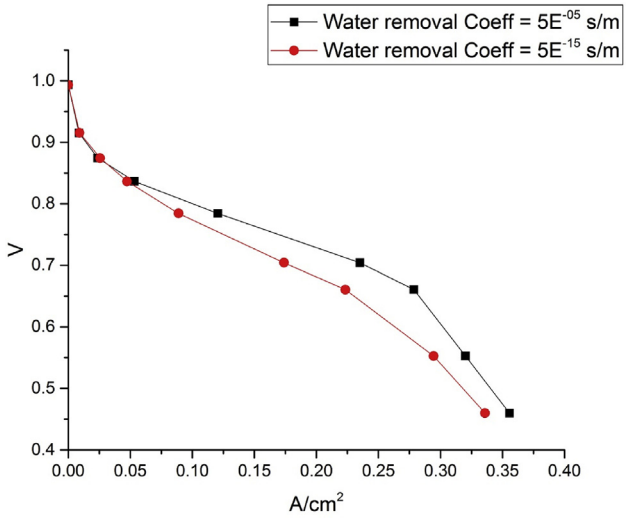

Fig. 9 – Comparison of simulated polarization curves for different values of water removal coefficient.

Fig. 10a–b depicts the liquid water saturation distribution at GDL and channel interface on the cathode side for two different values of the coefficient of liquid removal. For the low value of water removal coefficient (5 E^{-15}s/m), the liquid saturation at GDL and channel interface has a maximum value of 0.22 which is very high compared to the high value of water removal coefficient (5 E^{-05} s/m) which is 0.0053. It means that the electrode and GDL pores for the case of the low value of the coefficient of liquid removal are more clogged than the high liquid removal rate case.

Fig. 11a–b presents the distribution of oxygen mass fraction at catalyst and membrane interface on the cathode. The maximum value of the mass fraction of oxygen for the high value of the coefficient of liquid removal (5 E^{-05} s/m) is 0.16 while in the case of the low-value coefficient of liquid removal (5 E^{-15} s/m) it is 0.154. This reduction in the oxygen concentration is due to the increase of concentration losses because of electrodes and GDL pores blockage by liquid water.

Matching simulated and experimental curve

Matching procedure

In the modelling of PEM fuel cells, matching of the simulated and experimental curve is an essential step as this provides the best-fit values of input parameters to the model that cannot usually or readily be found independently by experiment. By applying the model with these inputs to a number of cases (e.g. different operating conditions) in which their values would not be expected to change and checking that the simulated curve still matches the modified experimental curve.

The matching of simulated and experimental polarization curves is in practice a challenging process because the precise numerical values of key model input parameters – such as exchange current densities, charge transfer coefficients, specific active surface areas, local species concentrations, condensation rate, and water removal coefficient – are not available through independent experiments. Hence these input parameters are used as fitting variables to get a close match between the simulated and experimental curve, which is a time-consuming practice. A step-by-step procedure thus needs to be developed, to allow matching of the simulated and experimental polarization curves within as short a computing time as possible.

In this section, each polarization region of experimental curve-1 (Fig. 12) obtained from the testing of the 5 cm^2 parallel-channel URFC operating at specified conditions (that is, relative humidity and cell temperature) were matched with the simulated polarization curve based on the findings in section The influence of input parameters on a polarization curve. After that to check the uniqueness of the values of the best-fit input parameters, a second simulation curve was compared with experimental curve-2 (Fig. 12) obtained from the testing of the same 5 cm^2 parallel-channel URFC but operating at different conditions (see Table 4) A close

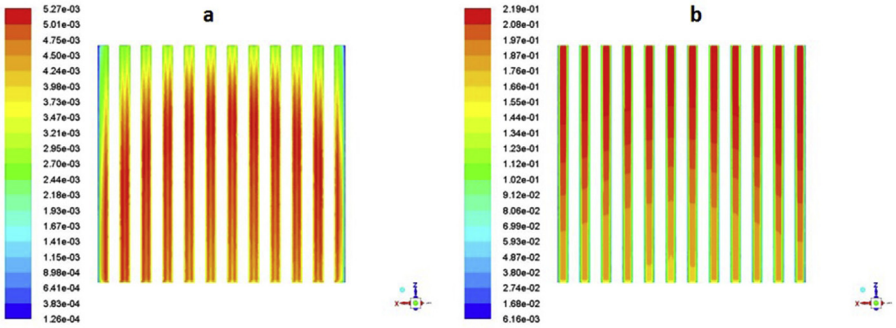

Fig. 10 – Water saturation distribution on the cathode GDL/channel interface at 0.46 V of; a) water removal coefficient = 5 E^{-05} s/m and b) water removal coefficient = 5 E^{-15} s/m.

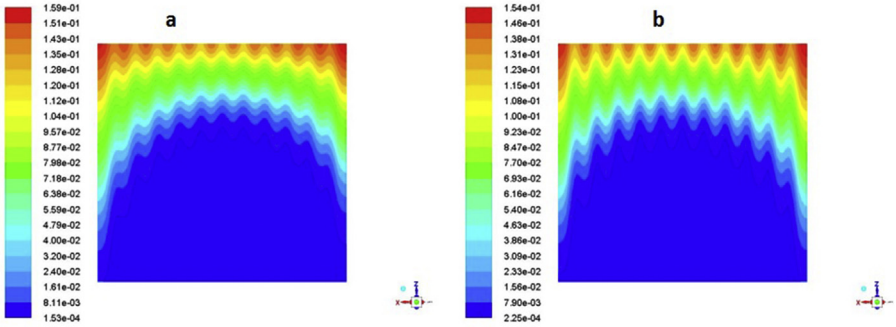

Fig. 11 – Oxygen mass fraction distribution on the cathode GDL/channel interface at 0.46 V of; a) water removal coefficient = 5 E^{-05} s/m and b) water removal coefficient = 5 E^{-15} s/m.

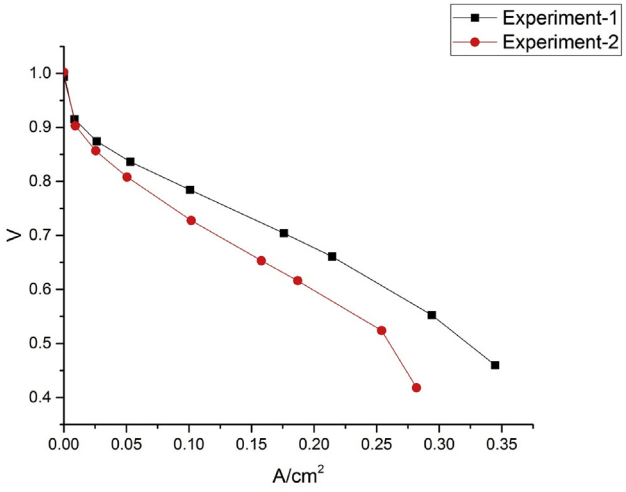

Fig. 12 – Experimental curves for different operating conditions.

agreement was found between both curves by keeping the entire model input parameters the same as for the getting fit for the experimental curve-1 while changing the operating conditions.

Matching in activation polarization region

The process of the matching simulated curve with experimental started with getting a better fit in the activation polarization region. Based on the observation made in the earlier section, it was found that the activation loss region is influenced mainly by changing the values of exchange current densities and charge transfer coefficients. So, in the first step, initial values for j_a and j_c were set at 50 A/m^2 and 5 A/m^2 respectively. When the simulation output values of current densities were plotted against voltage and compared with experimental polarization curve as displayed in Fig. 13, it was found that there was no match between two curves in any region.

In the second step, the values of j_a and j_c were raised to 100 A/m^2 and 10 A/m^2 respectively to get a lift in the activation polarization region. By comparing simulation polarization curve with experimental as shown in Fig. 14, it is observed

Table 4 – Operating conditions of different experiments.

Experiment	Relative Humidity on Air Side	Relative Humidity on Hydrogen Side	Cell Temperature
1	34%	66%	53 C°
2	48%	78%	55 C°

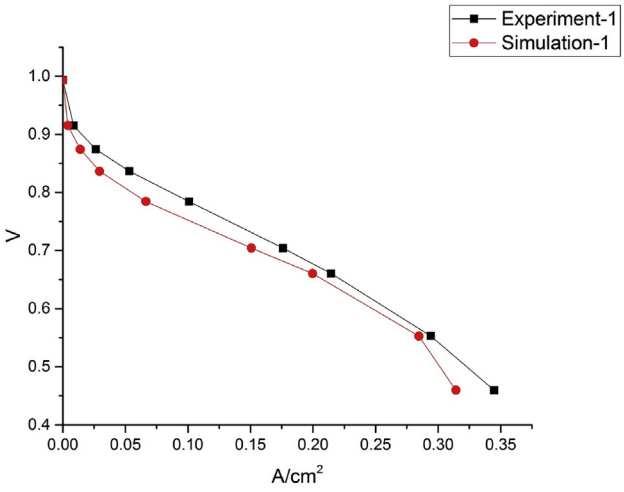

Fig. 13 – Comparison of experimental polarization curve and simulation polarization curve for set-1 values.

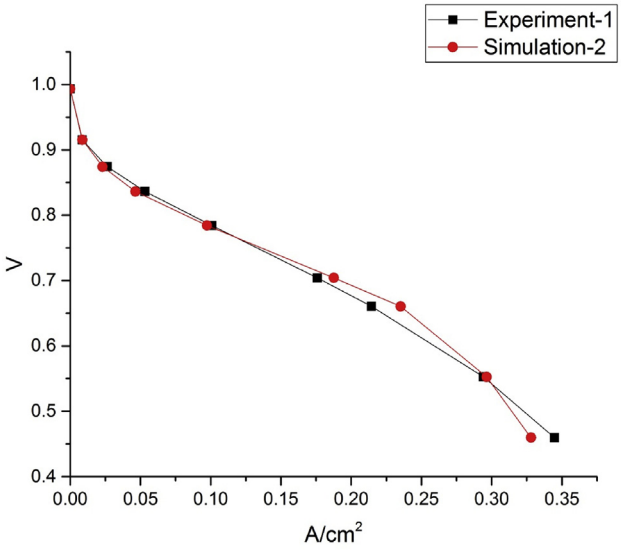

Fig. 14 – Comparison of experimental polarization curve and simulation polarization curve for set-2 values.

that there was a relatively a good fit between the two curves in the activation polarization region, but the slope of the simulation curve is more than that of experimental.

Based on the findings in section Charge transfer coefficients, the value of charge transfer coefficient at the cathode electrode was then tuned to reduce the slope of the curve in the activation losses region. As it was observed in section Charge transfer coefficients the charge transfer coefficients values for the anode electrode have less influence on the overall polarization curve, so for the sake of reducing fitting variable the value for charge transfer coefficient for anode electrode was kept constant. In this step, the value of the charge transfer coefficient at the cathode was raised from 0.60 to 0.65. As can be seen in Fig. 15, both curves are now closely matched in activation loss regions.

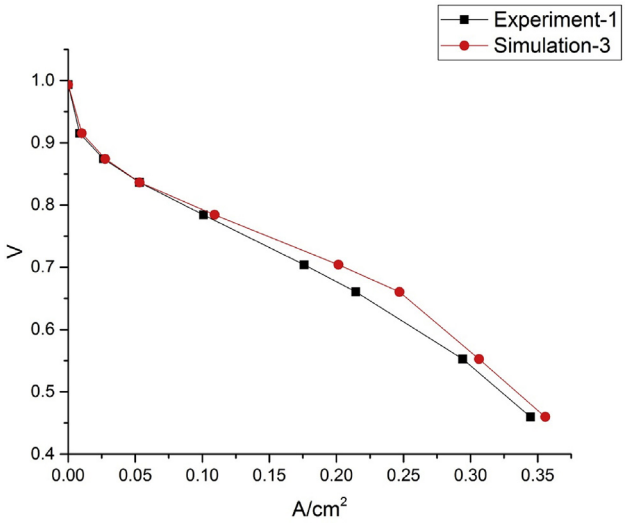

Fig. 15 – Comparison of experimental polarization curve and simulation polarization curve for set-3 values.

Matching in ohmic polarization region

As discussed in sections Protonic conduction coefficient and Contact resistance, the ohmic loss region is influenced by the values of proton conductivity coefficient and contact resistance. The value of the proton conductivity coefficient was set one from the beginning. Two criteria were used to check the value of the proton conductivity coefficient was within the appropriate range. Firstly, the membrane conductivity was calculated using Eq. (5) from the simulation data and then compared with the value of proton conductivity reported in the literature. According to the literature, the membrane conductivity for Nafion 115 at room temperature is reported to be 0.095 S/cm [40]. The calculated value of membrane conductivity based on the simulation data is 0.090 S/cm, which is closer to the value reported in the literature. Secondly, the membrane resistance was calculated and compared with the value of total cell resistance. The value for the membrane resistance comes out to be 41 mΩ while the total cell resistance is 61 mΩ, which is higher than the membrane resistance means that the rest of resistance is due to the contact resistance of PEM Fuel cell components. The value for the contact resistance between components of PEM Fuel cell was calculated by subtracting membrane resistance from the total cell resistance and was fed in as an input value. Hence the values for proton conduction coefficient and contact resistance were set based on the experimental data.

Matching in concentration polarization region

As shown in Fig. 15, the simulation curve overestimates the experimental curve in the ohmic and concentration polarization regions. The value for protonic conduction coefficient and contact resistivity were set based on the value of total cell resistance (section Matching in ohmic polarization region). It

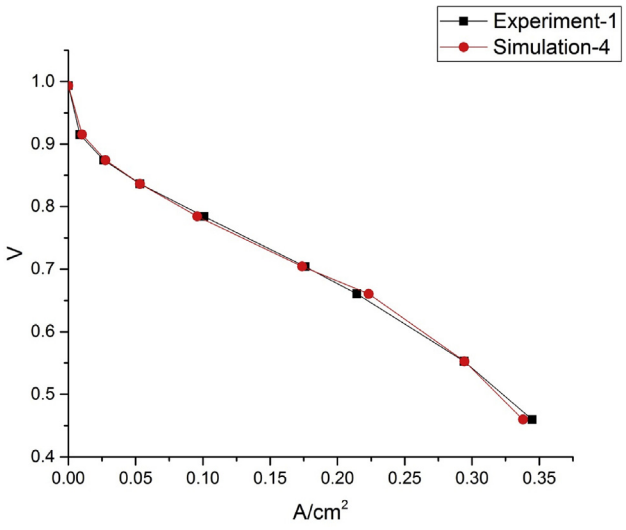

Fig. 16 – Comparison of experimental polarization curve and simulation polarization curve for set-4 values.

Table 5 – Sets of input parameter values for different simulations.

Simulation	J_a (A/m^2)	J_c (A/m^2)	α_a	α_c	β	Θ (s/m)	$\dot{r}$ (Ω-m^2)
1	50	5	0.6	0.6	1	5E^{-05}	11.5 E^{-06}
2	100	10	0.6	0.6	1	5E^{-05}	11.5 E^{-06}
3	100	10	0.6	0.65	1	5E^{-05}	11.5 E^{-06}
4	100	10	0.6	0.65	1	5E^{-15}	11.5 E^{-06}

is assumed that the simulation curve overestimates the experimental curve because the experimental curve has more concentration losses than the simulation curve. The value of water removal coefficient was thus reduced from 5 E^{-05} s/m to 5 E^{-15} s/m to increase the concentration losses in the simulation curve. Because of that, more liquid water was trapped in GDL and electrode pores due to which the flow of oxidant was restricted. The ohmic and concentration polarization regions of the simulation and experimental curves are now reasonably matched, as depicted in Fig. 16. This shows that concentration losses start their effects at medium current densities but get more severe at high current densities.

The values of input parameters that were used from simulation 1 to simulation 4 are listed in Table 5.

As it can be seen in Eqs. (7) And (8), terms like; r_s and γ_j can also influence the concentration polarization regions. But since our test cell is generating less current due to which the value of liquid saturation is low. In our earlier work through independent runs, it was found that due to low value of liquid saturation "s", the variation of values of exponent of pores blockage have a little effect on the mass transport losses region of the polarization curve. Similarly, it was also found that due to low value of liquid saturation "s" the reduction in performance of PEMFC due to covering of active sites of catalyst surface is negligible.

Hence the degree of effect of the exponent of pores blockage and exponent of reduction in the catalyst effective area on the mass transport losses region of the polarization curve were relatively small than the coefficient of liquid removal that is why we have only focused on the coefficient of liquid removal to get fit in the concentration polarization region.

Evaluating closeness of fit

The closeness of fit between simulated and experimental curve was evaluated by using different statistical criteria, namely: percentage difference (between current density points on simulated and experimental curves at a given cell voltage), mean squared difference, sum of squared differences, and coefficient of determination (R^2). Initially, percentage differences values were calculated for all voltage points of each simulation, as shown in Table 6. The maximum acceptable percentage difference value was kept at 5%. The values of mean squared difference, sum of squared differences, and coefficient of determination (R^2) are shown in Table 7.

If it emerged that the fit obtained by tuning exchange current densities, charge transfer coefficients, protonic conduction coefficient and was still insufficiently close, it is important to note that there are also other numerical input parameters in the Module that may also be varied to improve the match. These additional parameters include most notably: exponent of pore blockage concentration dependence, and local species concentration reference values.

Checking the uniqueness of input parameters

After getting closer fits in all the regions, the next step was to make sure that the values of exchange current densities, charge transfer coefficients and coefficient of liquid removal that was used for getting closer fit are unique values. Simulation polarization curve-using the same values of exchange current densities, charge transfer coefficients, and coefficient of liquid removal were therefore compared with experimental curve for the same cell operating under different conditions, specifically a different cell temperature and relative humidity. While the difference in temperature between experiment 1 and 2 is only 2 C°, but Relative humidity difference is much larger at 14% for air and 12% for the hydrogen. Hence this degree of difference between the cases is more than enough to give a clear difference in performance (as can be seen in Fig. 12), and thus a sufficient test of the ability of the model with the 'best-fit values' of input parameters, and just these changes in operating conditions, to represent both conditions with reasonable accuracy. A similar procedure was also suggested by Ref. [32] for checking the uniqueness of the values of input parameters. This procedure was also followed by Hu et al. [41] to check the accuracy of the model by comparing the numerical polarization curve using the same values of exchange current densities with the experimental polarization curve at different operating pressure.

The comparison is shown in Fig. 17 and indicates a close fit in all three regions of polarization curve. This closeness of fit indicates strongly that the values of exchange current densities, charge transfer coefficients, and water removal coefficient found reflect the properties of the cell itself and hence apply equally under different cell operating conditions. While this fit does not exclusively prove that the solution set for

Table 6 – Values of percentage errors for different simulated curves.

Voltage (V)	Percentage Differences			
	Simulation-1 (%)	Simulation-2 (%)	Simulation-3 (%)	Simulation-4 (%)
0.993	0	0	0	0
0.915	−148	−15	3	3
0.874	−88	−14	5	5
0.836	−80	−15	0.3	0.3
0.784	−52	−4	8	−5
0.704	−17	6	13	1
0.661	−7	9	13	4
0.553	−3	1	4	0.1
0.460	−10	−5	3	−2

Table 7 – Values of mean squared difference, sum of squared differences and coefficient of determination for all simulations.

Simulation	Mean Squared difference	Sum of Squared differences	R^2
1	$2.74\ E^{-03}$	$2.5\ E^{-02}$	0.81
2	$1.30\ E^{-06}$	$1.00\ E^{-05}$	0.96
3	$9.26\ E^{-04}$	$8.33\ E^{-03}$	0.93
4	$1.0\ E^{-06}$	$9.50\ E^{-06}$	0.99

these input parameters found is unique, the probability of this not being the case is low. This probability of error in the solution set is reduced further if additional simulations with these inputs of the cell operating under different conditions again do not reveal significant differences between the resulting simulated and experimental curves.

Step-by-step procedure

In this section, the procedure used to match a simulated and an experimental polarization curve for a PEM fuel cell is generalised into a step-by-step procedure that can be applied to any particular case. The overall procedure is shown as a flow diagram in Fig. 18.

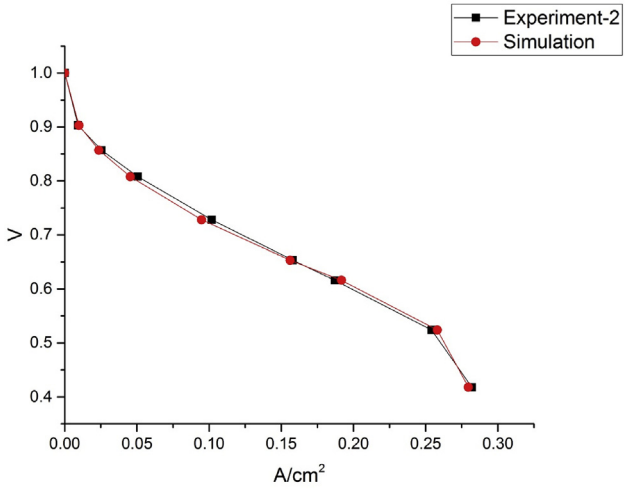

Fig. 17 – Comparison of experimental polarization with different operating conditions curve and simulation polarization curve for set-4 values.

The first step is to get a good fit in the activation polarization region (top box in Fig. 18). As discussed in sections Charge transfer coefficients and Exchange current densities, exchange current densities and charge transfer coefficients are the main input parameters that influence the curve in the activation polarization region. Initially, starting values for j_a, j_c, α_a and α_c are chosen and two voltage points in the activation polarization region are simulated. The value of j_a should be between 10^1 and 10^4 times that of j_c, as explained in section Exchange current densities.

Once the first simulation run is completed, the values of current density at the anode catalyst and membrane interface, with the cathode catalyst and membrane interface, are compared. If both values are equal, then keep the same ratio of j_a to j_c else change the ratio. After that, the current densities in the activation polarization regions obtained from the simulation and experimental data are compared. If they are close enough, tuning the values of j_a and j_c is stopped; if the values are not close, then the values of j_a and j_c are increased or decreased by some specific percentage (e.g. 10%, 20%, etc) according to the difference between simulated and experimental values. The tuning of exchange current densities can be stopped when the simulated and experimental curves get closer in the activation polarization region. In the next step, the slopes of the simulated and experimental curve should be compared. The slopes of the two curves can be matched by changing the value of charge transfer coefficients at the cathode side. As it was found in section Charge transfer coefficients, the values of current densities are more sensitive to change of the values of charge transfer coefficients on the cathode side only. Once the activation regions of both curves get a reasonably good match, then these parameters should be kept fixed for the next simulations. It was found in the present case that $j_a = 100\ A/m^2$ and $j_c = 10\ A/m^2$ give a closer fit in the activation region, but there was still a difference in the slope of both curves. The value of the charge transfer coefficient on the cathode side was increased from 0.6 to 0.65 to match the slopes of both curves. Variation of values of exchange current densities and charge transfer coefficients can give fit in the activation polarization region.

Ohmic losses region of the polarization curve can be fitted by varying the value of the protonic conduction coefficient (middle box in Fig. 18). The starting value for running the

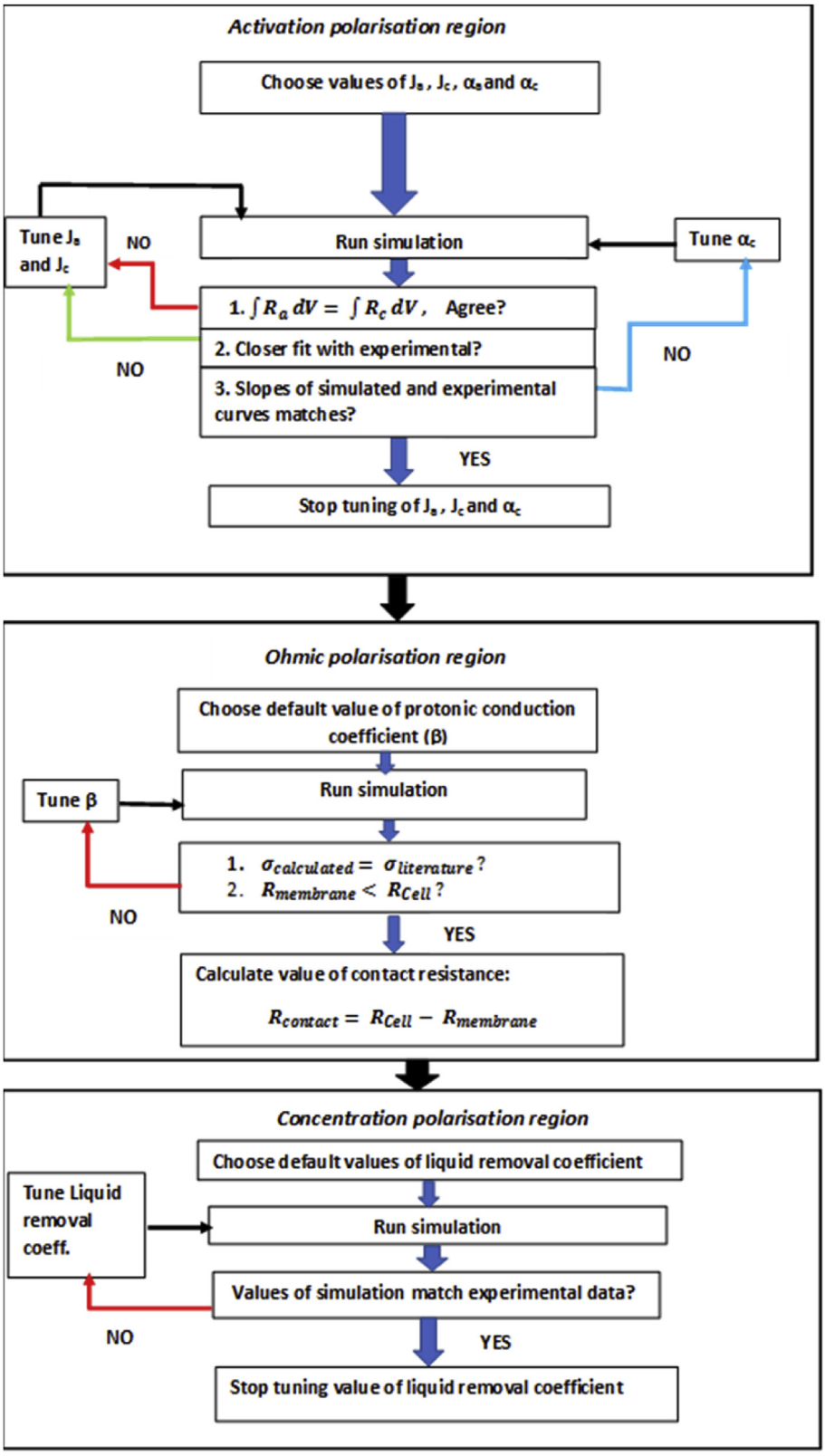

Fig. 18 – Flow diagram of the step-by-step procedure.

simulation is always the default value of the protonic conduction coefficient. The value of membrane conductivity is calculated using Eq. (5) based on the values of simulation output data. If the value of the simulated membrane conductivity matches the values of membrane conductivity in the literature, and the membrane resistance is less than the total cell resistance, then the default value of protonic conduction coefficient can be fixed for the next simulation.

Otherwise the value of protonic conduction coefficient is tuned until it meets the two criteria. The values of contact resistance can be calculated by subtracting membrane resistance from the total cell resistance. In our case, the default value – i.e.: 1 – of protonic conduction coefficient satisfied the criteria mentioned above, so the value of protonic conduction coefficient was kept constant in all simulations.

The concentration losses in the PEM fuel cell depend on the amount of liquid water present in the PEM fuel cell (bottom box in Fig. 18). The liquid water removal rate can vary the amount of liquid water present in the fuel cell: the lower the assumed rate, the more water remains in the cell. The water removal coefficient can be used as a fitting parameter to match the simulated and experimental curves in the concentration region. The values of the current densities in the activation and ohmic polarization regions will not be affected significantly by varying the value of the coefficient of the liquid water.

With the default value of water removal coefficient (5 E^{-05} s/m), the simulated polarization curve overestimated the experimental polarization curve. By decreasing the value of water removal coefficient to 5 E^{-15} s/m, more water will clog the GDL pores, and less oxidant will reach the catalyst for electrochemical reaction. By comparing Figs. 15 and 16, it can clearly be observed that concentration losses start at medium current densities but get more severe at higher current densities.

As mentioned in section Evaluating closeness of fit, there are also some other input parameters in the ANSYS PEM Fuel Cell Module – like: exponent of pore blockage, concentration dependence, local species concentration reference values –, that can be varied to get a match between simulated and experimental polarization curves but tuning all of them to get the fit between the two curves will increase the computational time. The average time taken for a solution to be converged in this study was 4 hours for each voltage point. Hence tuning only the primary input parameters (charge transfer coefficients, exchange current densities, protonic conduction coefficient, and coefficient of liquid removal) can match simulated and polarization curve with less computational time. If the closeness of fit is still less than required, additional parameters can also be tuned.

Discussion

Matching a simulated and experimental polarization curve is a time-consuming practice if a systematic procedure is not followed. The systematic step-by-step procedure presented in this paper can substantially reduce the research personnel, and computer time, required to achieve this match.

The procedure relies on an understanding of how different input parameters influence the polarization curve in its three regions to varying degrees. However, tuning one parameter at a time can improve the fit in one polarization region, but it may worsen it in the other regions. For example: by varying value of liquid removal coefficient can fit the concentration losses region but may miss-match the already fitted values in the ohmic polarization region. Hence overall some degree of iteration of all the input parameters is required to obtain the optimal solution set.

The closeness of the fit between simulated and experimental polarization curves may initially be assessed by visual inspection, but as the match improves quantitative statistical criteria must be used, such as mean squared difference, sum of squared differences, and coefficient of determination (R^2). As shown in Table 6, the maximum percentage difference between simulation and experimental values in the example presented in this paper for simulation 4 is ± 5%, and this difference was progressively reduced with each simulation conducted. The fit is said to be perfect if the value of the sum of squared differences is zero and R^2 is one [42]. From Table 7, the values of the sum of squared differences and R^2 for simulation-4 are 9.50 E^{-06} and 0.99, respectively, which are very close to the ultimate limit.

The selected set of input parameters has been calibrated on the basis of their physical significance in the different polarization regions of the polarization curve. Driven by the physical meaning of the set of parameters, it poses dominant effects on the polarization curve compared to others. Hence the values of these parameters have been calibrated within an acceptable physical range to achieve a close agreement with the experimental measurements. Without a solid theory deviation or experimental measurement, these parameters should not be calibrated. So, the focus of this paper is on a systematic approach to capture the system performance with physical consideration.

If necessary, the values of the maximum percentage difference can be further reduced, by tuning other input parameters that have so far been kept constant, including the exponent of pore blockage concentration dependence, and local species concentration reference values.

In the present work, this step-by-step procedure has been implemented manually, with each set of input parameters fed into the model, and the resulting polarization curve compared with the experimental curve outside of the model itself. It is noteworthy, however, that the entire step-by-step matching procedure can be converted into an algorithm and incorporated into an expanded simulation model, which then systematically sought the best fit in terms of say coefficient of determination (R^2) by tuning all the input parameters. In this systematic procedure there will be always an opportunity to expand this procedure to all the input parameters that have values that cannot be found independently before the simulation.

In a complex model of a fuel cell such the ANSYS PEM Fuel Cell Module and other similar softwares, with a multiplicity of input parameters that cannot be determined directly and individually by experiment, it is always possible that the solution set found that gives a close fit to an experimental curve is not unique. To test for uniqueness, the best course of action is to run the model for a particular cell with fixed characteristics, and hence by expectation a unique set of input parameters that define these characteristics, under several different experimental conditions, to check that the best-fit set of input parameters does not change significantly. Of course, it is always important to look for experiments that can independently measure these values, or at least indicate a

likely range for these. For example, accurate data on the voltage – current density relationship at very low currents can give ranges for the values of the charge transfer coefficient and exchange current density for the cathode via Tafel plots. But a Tafel plot assumes only the cathode has a significant overpotential, with the anodic overpotential assumed negligible. In practice the latter can be significant [43], so there will be some error in the cathodic charge transfer coefficient and exchange current density thereby estimated. Moreover, the Tafel plot gives no information on the corresponding anodic values.

Cells with the same MEAs should have the same exchange current densities, even if the flow channel configurations varied, or the cells are operated under different operating conditions.

It remains important to be aware that, due to the multiplicity of numerical input parameters in a model such as the ANSYS Fuel Cell Module, a closer agreement between a simulated and experimental curve does not guarantee that the solution set for these input parameters is unique. But the probability of this not being the case is reduced if additional simulations of the cell operating under different conditions continue to show close agreement between the simulation and experiment. As shown in the additional simulation (Fig. 17), under different operating condition, the model was able to capture the system characteristics working under different operating conditions.

The step-by-step procedure explained here can be applied to any PEM fuel cell to match a simulated and experimental polarization curves and hence calibrate the model. Once the best fit values for the input parameters are found or the model has been calibrated, under particular set of operating conditions like; operating temperatures, relative humidities and gasses mass flow rates, this model maybe used to predict the performance of the same cell under different operating conditions.

Conclusion

This paper has highlighted the input parameters that are influencing the different polarization regions of the PEM fuel cell polarization curves. It was found that exchange current densities and charge transfer coefficients mainly control the activation losses in the PEM fuel cell. To match the activation losses region of the simulation and experimental polarization curve, these two input parameters should first be tuned. The key factors responsible for the ohmic losses are membrane resistance and contact resistance. Membrane protonic conduction coefficient value can be tuned to increase and decrease the value of the membrane conductivity to get the fit between experimental and simulation polarization curves in the ohmic polarization region. The water removal coefficient influences mass transport losses: the higher its value, the less will be the concentration losses at higher current densities. The value of the water removal coefficient can be adjusted to get the sharp turn down in the mass transport losses region at high current densities. It was also observed that the concentration losses begin at medium current densities and get more critical as current densities increases.

A step-by-step procedure has been developed to match simulated and experimental polarization curves and shown to work effectively for the case of a single PEM fuel cell under two sets of operating conditions. The same best-fit values for key input parameters defining the properties of the cell itself were used under both conditions, and a close match between simulated and experimental curves was found. This lends support to the uniqueness of the best-fit solution set. In applying this procedure in practice, it may be necessary to undertake further checks of the uniqueness of the solution by, for example, comparing the simulated and experimental polarization curves for two cells with the same MEA and GDLs (and hence many of the same input parameters) but with different flow channel configurations.

In future, this systematic procedure may be incorporated as an algorithm within an expanded simulation package, which then automatically and systematically seeks the best fit, in terms of say coefficient of determination (R^2), by tuning all the input parameters.

The findings of this study can further contribute to using comprehensive computer simulation models of PEM fuel cells, such as the ANSYS PEM Fuel Cell Module, as a tool for optimising the design of PEM fuel cells – for example, the optimal flow channel configuration, and membrane electrode assembly and GDL characteristics – and diagnosing areas of poor performance of a particular cell. This procedure may also be extended in the future to modelling fuel cell stacks.

Acknowledgements

The authors are grateful to the members of the Reversible Fuel Cell team in the School of Engineering at RMIT University for use of data on the performance of a single-cell PEM URFC; and for the general funding support for URFC development received from the Australian Department of Defence through the Defence Science Technology Group for the Capability Technology Demonstrator project, "The development and demonstration of a low signature, rechargeable and portable energy supply using reversible hydrogen fuel cells to support forward operating bases" (2015–2017; grant number CTD 2014-3).

Nomenclature

j	Reference exchange current density per active surface area
ζ	Specific active surface area
[], $[]_{ref}$	Local species concentration, reference value
γ	Concentration dependence exponent
α	Charge transfer coefficient
R	Universal gas constant
T	Temperature
F	Faraday constant
σ	Electrical conductivity
ϕ	Electric potential
R	Volumetric transfer current
β	Protonic conduction coefficient

ω	Protonic conduction exponent
E	Activation energy
λ	Water content
M	Molecular mass
D	Gas species diffusivity
s	Liquid saturation
r	Exponent of pore blockage
ε	Porosity
f	Flux
Θ	Liquid removal coefficient
p	Pressure
ρ	Density
V	Velocity
$\dot{r}$	Contact resistivity

Subscripts

an	Anode
cat	Cathode
ref	Reference
sol	Solid
mem	Membrane
w	Weight
H_2O	Water
eff	Effective
liq	Liquid water
c	Capillary

Appendix A. Supplementary data

Supplementary data to this article can be found online at https://doi.org/10.1016/j.ijhydene.2019.11.057.

REFERENCES

[1] Strachan N, Foxon TIM, Fujino J. Policy implications from the Low-Carbon Society (LCS) modelling project. Clim Policy 2008;8(1):S17–29.

[2] Luo X, Wang J, Dooner M, Clarke J. Overview of current development in electrical energy storage technologies and the application potential in power system operation. Appl Energy 2015;137:511–36.

[3] Chen H, Cong TN, Yang W, Tan C, Li Y, Ding Y. Progress in electrical energy storage system: a critical review. Prog Nat Sci 2009;19(3):291–312.

[4] Staffell I, Scamman D, Velazquez Abad A, Balcombe P, Dodds PE, Ekins P, Shah N, Ward KR. The role of hydrogen and fuel cells in the global energy system. Energy Environ Sci 2019;12(2):463–91.

[5] Hosseinzadeh E. Modeling and design of hybrid PEM fuel cell systems for lift trucks. DTU Mechanical Engineering; 2012.

[6] Bednarek T, Tsotridis G. Issues associated with modelling of proton exchange membrane fuel cell by computational fluid dynamics. J Power Sources 2017;343:550–63.

[7] Iranzo A, Muñoz M, Rosa F, Pino J. Numerical model for the performance prediction of a PEM fuel cell. Model results and experimental validation. Int J Hydrogen Energy 2010;35(20):11533–50.

[8] Berning T, Djilali N. Three-dimensional computational analysis of transport phenomena in a PEM fuel cell - a parametric study. J Power Sources 2003;124(2):440–52.

[9] Kone J-P, Zhang X, Yan Y, Hu G, Ahmadi G. Three-dimensional multiphase flow computational fluid dynamics models for proton exchange membrane fuel cell: a theoretical development. J Comput Multiph Flows 2017;9(1):3–25.

[10] Bernardi MD, Verbrugge WM. A mathematical model of the solid-polymer-electrolyte fuel cell. J Electrochem Soc 1992;139(9):2477–91.

[11] Thomas FF, John N. Water and thermal management in solid-polymer-electrolyte fuel cells'. J Electrochem 1993;140(5):1218–25.

[12] Jung SY, Trung VN. An along-the-channel model for proton exchange membrane fuel cells. J Electrochem 1998;145(4):1149–59.

[13] Mazumder S, Cole JV. Rigorous 3-D mathematical modeling of PEM fuel cells – II. Model predictions with liquid water transport'. J Electrochem Soc 2003;150(11):A1510–7.

[14] Moein-Jahromi M, Kermani MJ. Performance prediction of PEM fuel cell cathode catalyst layer using agglomerate model. Int J Hydrogen Energy 2012;37(23):17954–66.

[15] Xing L, Mamlouk M, Scott K. A two dimensional agglomerate model for a proton exchange membrane fuel cell. Energy 2013;61:196–210.

[16] Limjeerajarus N, Charoen-Amornkitt P. Effect of different flow field designs and number of channels on performance of a small PEFC. Int J Hydrogen Energy 2015;40(22):7144–58.

[17] Macedo-Valencia J, Sierra JM, Figueroa-Ramírez SJ, Díaz SE, Meza M. 3D CFD modeling of a PEM fuel cell stack. Int J Hydrogen Energy 2016;41(48):23425–33.

[18] Heidary H, Kermani MJ, Prasad AK, Advani SG, Dabir B. Numerical modelling of in-line and staggered blockages in parallel flowfield channels of PEM fuel cells'. Int J Hydrogen Energy 2017;42(4):2265–77.

[19] Chowdhury MZ, Genc O, Toros S. Numerical optimization of channel to land width ratio for PEM fuel cell. Int J Hydrogen Energy 2018;43(23):10798–809.

[20] Havaej P, Kermani MJ, Abdollahzadeh M, Heidary H, Moradi A. A numerical modeling study on the influence of catalyst loading distribution on the performance of Polymer Electrolyte Membrane Fuel Cell. Int J Hydrogen Energy 2018;43(21):10031–47.

[21] Li S, Sundén B. Effects of gas diffusion layer deformation on the transport phenomena and performance of PEM fuel cells with interdigitated flow fields. Int J Hydrogen Energy 2018;43(33):16279–92.

[22] Carcadea E, Varlam M, Marinoiu A, Raceanu M, Ismail MS, Ingham DB. Influence of catalyst structure on PEM fuel cell performance – a numerical investigation. Int J Hydrogen Energy 2019;44(25):12829–41.

[23] Zalitis CM, Sharman J, Wright E, Kucernak AR. Properties of the hydrogen oxidation reaction on Pt/C catalysts at optimised high mass transport conditions and its relevance to the anode reaction in PEFCs and cathode reactions in electrolysers. Electrochim Acta 2015;176:763–76.

[24] Harvey D, Pharoah JG, Karan K. A comparison of different approaches to modelling the PEMFC catalyst layer. J Power Sources 2008;179(1):209–19.

[25] Ju H, Wang C-Y. Experimental validation of a PEM fuel cell model by current distribution data, vol. 151; 2004. p. A1954–60. 11.

[26] Lum KW, McGuirk JJ. Three-dimensional model of a complete polymer electrolyte membrane fuel cell – model formulation, validation and parametric studies. J Power Sources 2005;143(1):103–24.

[27] Mench MM, Wang CY, Ishikawa M. In: Situ current distribution measurements in polymer electrolyte fuel cells, vol. 150; 2003. A1052–9. 8.

[28] Ansys. ANSYS fluent fuel cell module manual. 2017.
[29] Wu X. The influence of active area and stacking on PEM fuel cell performance: a simulation modelling and experimental investigation. Doctor of Philosphy thesis. RMIT University; 2017.
[30] Arvay A, Ahmed A, Peng XH, Kannan AM. Convergence criteria establishment for 3D simulation of proton exchange membrane fuel cell. Int J Hydrogen Energy 2012;37(3):2482–9.
[31] Huang X, Zhang Z, Jiang. J 'fuel cell Technology for distributed generation: an overview, vols. 9–13; July 2006. p. 1613–8.
[32] Min CH, He YL, Liu XL, Yin BH, Jiang W, Tao WQ. Parameter sensitivity examination and discussion of PEM fuel cell simulation model validation: Part II: results of sensitivity analysis and validation of the model. J Power Sources 2006;160(1):374–85.
[33] Vetter R, Schumacher JO. Experimental parameter uncertainty in proton exchange membrane fuel cell modeling. Part II: sensitivity analysis and importance ranking. J Power Sources 2019;439:126529.
[34] Zhao D, Dou M, Zhou D, Gao F. Study of the modeling parameter effects on the polarization characteristics of the PEM fuel cell. Int J Hydrogen Energy 2016;41(47):22316–27.
[35] Biaku CY, Dale NV, Mann MD, Salehfar H, Peters AJ, Han T. A semiempirical study of the temperature dependence of the anode charge transfer coefficient of a 6kW PEM electrolyzer. Int J Hydrogen Energy 2008;33(16):4247–54.
[36] Tijani AS, Binti Kamarudin NA, Binti Mazlan FA. Investigation of the effect of charge transfer coefficient (CTC) on the operating voltage of polymer electrolyte membrane (PEM) electrolyzer. Int J Hydrogen Energy 2018;43(19):9119–32.
[37] Soderberg JN, Co AC, Sirk AHC, Birss VI. Impact of porous electrode properties on the electrochemical transfer coefficient. J Phys Chem B 2006;110(21):10401–10.
[38] Larminie James DA. Fuel cell systems explained. 2nd ed. England: John Wiley & Sons Ltd; 2003.
[39] Mishra V, Yang F, Pitchumani R. Measurement and prediction of electrical contact resistance between gas diffusion layers and bipolar plate for applications to PEM fuel cells. J Fuel Cell Sci Technol 2004;1(1):2–9.
[40] Lufrano F, Staiti P, Minutoli M. Influence of nafion content in electrodes on performance of carbon supercapacitors. J Electrochem Soc 2004;151(1):A64–8.
[41] Hu M, Gu A, Wang M, Zhu X, Yu L. Three dimensional, two phase flow mathematical model for PEM fuel cell: Part I. Model development. Energy Convers Manag 2004;45(11):1861–82.
[42] Sayad DS. Model evaluation – regression. 2019. viewed 25/05/2019, https://www.saedsayad.com/model_evaluation_r.htm.
[43] Doddathimmaiah A, Andrews J. Theory, modelling and performance measurement of unitised regenerative fuel cells. Int J Hydrogen Energy 2009;34(19):8157–70.